Supporting Information

High Performance, Binder-free, Electrodes with Single Atom Catalysts on Doped Nanocarbons for Electrochemical Water Splitting Synthesized using One-Step Thermally-Controlled Delamination of Thin Films

Efrat Shawat Avraham[a#], Bibhudatta Malik[a#], Alina Yarmolenko[a#], Rajashree Konar [a,b], Sergei Remennik[c], Gili Cohen Taguri[a], Sandro Zorzi[d], Elti Cattaruzza[d], Michael Yakov Hubner [a], Gilbert Daniel Nessim[a]*

[a] Department of Chemistry and Institute of Nanotechnology and Advanced Materials (BINA), Bar-Ilan University, Ramat-Gan 5290002, Israel

[b] Atomic Structure-Composition of Materials, INL - International Iberian Nanotechnology Laboratory, Avenida Mestre José Veiga s/n4715-330, Braga, Portugal

[c] Center for Nanoscience and Nanotechnology, Hebrew University, Jerusalem 9190401, Israel

[d] Department of Molecular Sciences and Nanosystems, "Università Ca' Foscari Venezia", Via Torino 155, 30172 Venezia Mestre, Italy

 # Authors have equal contributions to this work

Corresponding author's Email: gdnessim@biu.ac.il

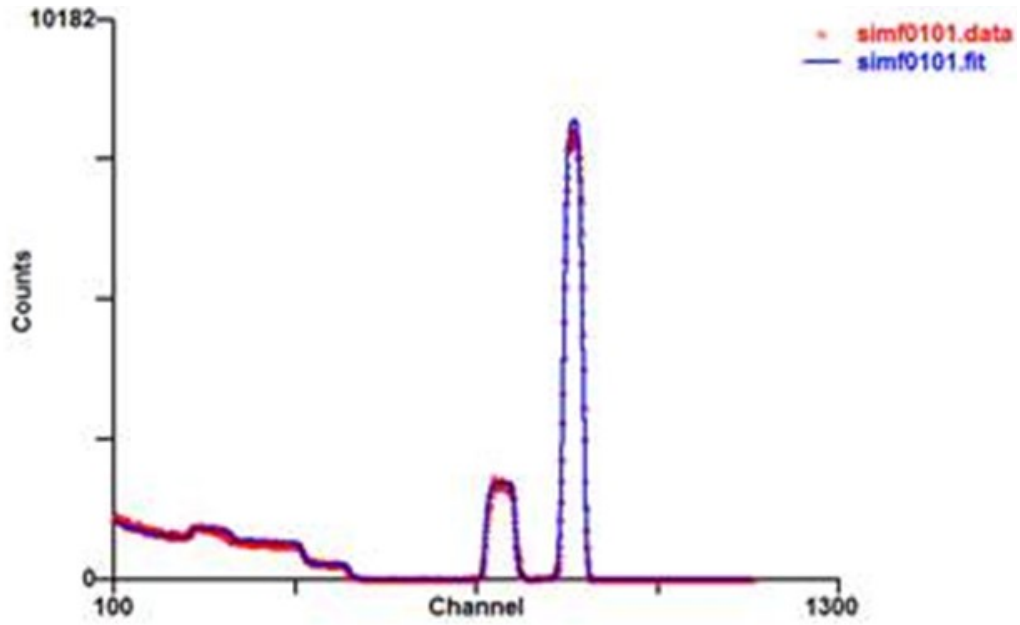

Layer	t (1e15at/cm2)	t (nm)	r(1e22at/cm3)	ni	au	si1o2	si
1	777.257	85.179	9.125	100.0000	0.0000	0.0000	0.0000
2	288.045	48.788	5.904	0.0000	100.0000	0.0000	0.0000
3	2164.229	310.243	6.976	0.0000	0.0000	100.0000	0.0000
4	25000.000	5023.106	4.977	0.0000	0.0000	0.0000	100.0000

Fig. S1. *Rutherford backscattering (RBS) analysis confirms the thickness of the different layers of the thin film stack deposited using e-beam evaporation.*

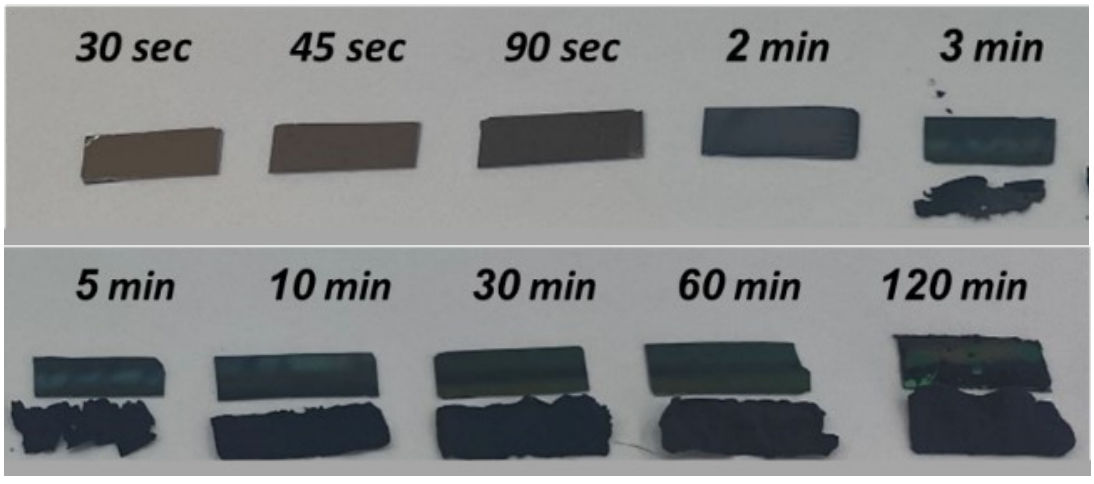

Fig. S2 *Images of sulfur-doped electrodes synthesized for growth times from 30 sec to 120 min. We can see growth of the nanocarbon-based electrode starting at 3 min.*

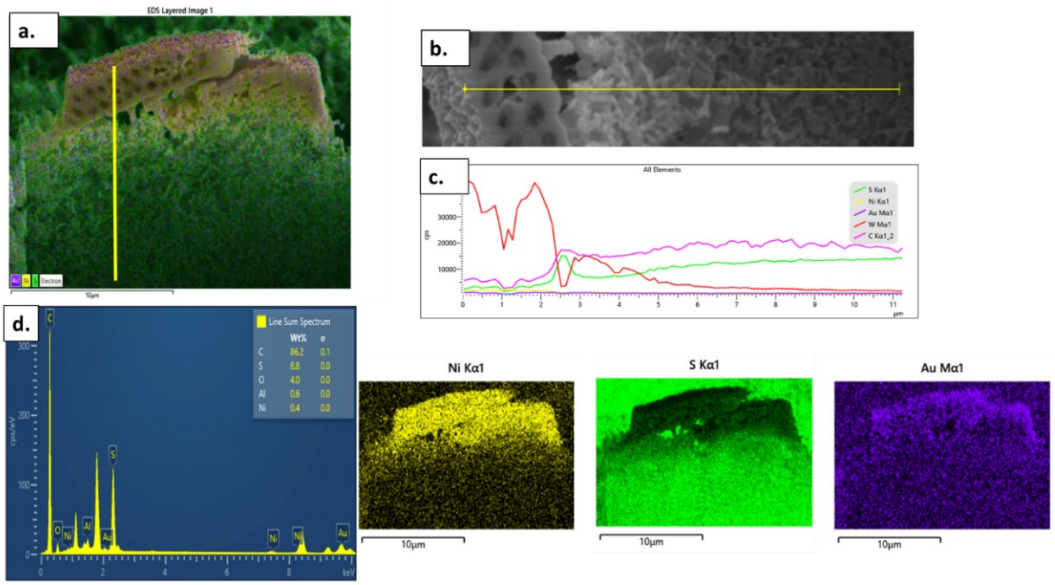

Fig. S3 *(a) FIB image with EDAX mapping following the line across the sample with (b) higher magnification. Note that the top surface of the electrode is at the bottom in (a) and at the right in (b). (c) Atomic percentage of the elements across the sample as we go towards the top surface. (d) Average EDAX values in the cross-section.*

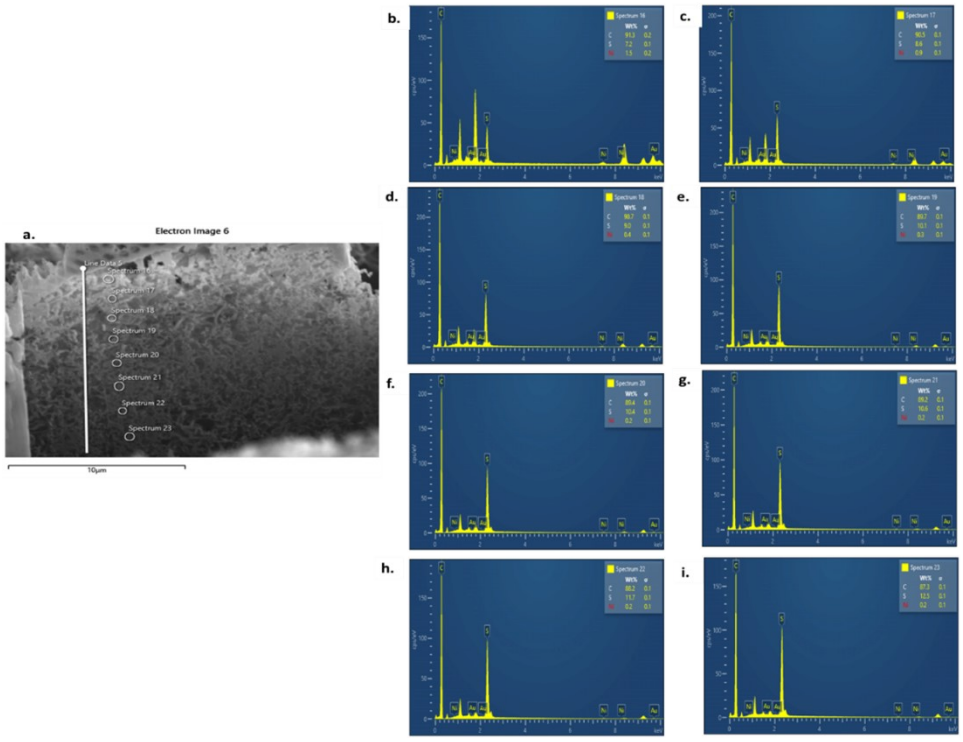

Fig. S4. *(a) EDAX mapping on the FIB cross-section at different points of the nanocarbon-based electrode. (b-i) spectra 16-23 show the amount of carbon and nickel*

at the different points in (a) moving towards the top surface of the electrode. The Ni content decreases towards the top surface in correlation with XPS which could not detect nickel on the top surface (SACs are below the XPS detection limit).

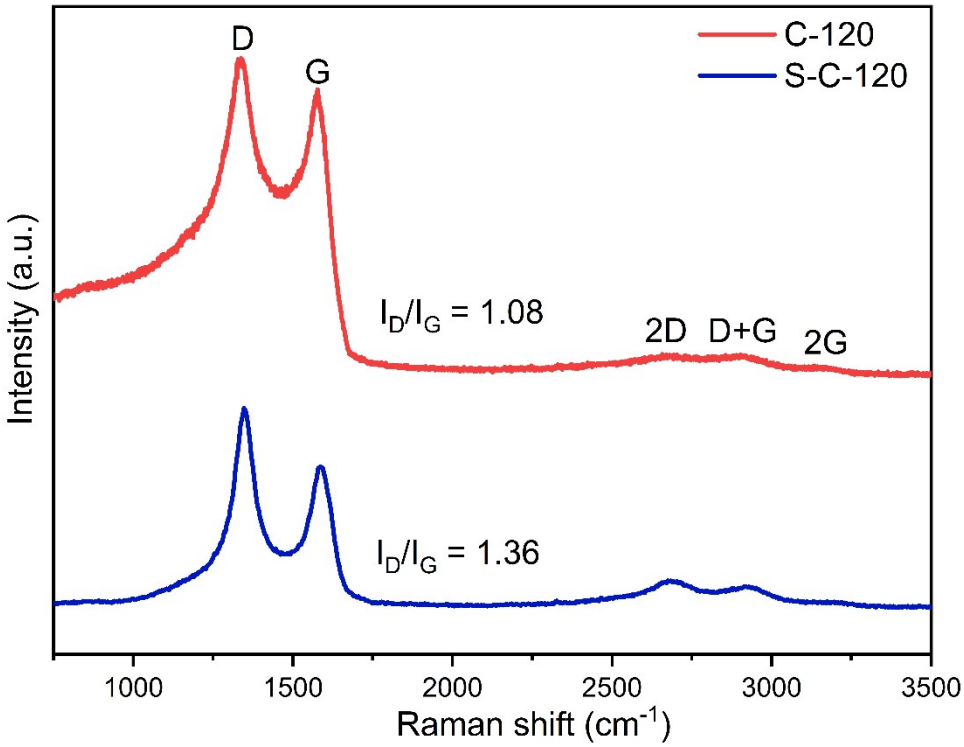

Fig. S5. *Raman spectroscopy of S-C-120 (sample 1) and C-120 (sample 2).*

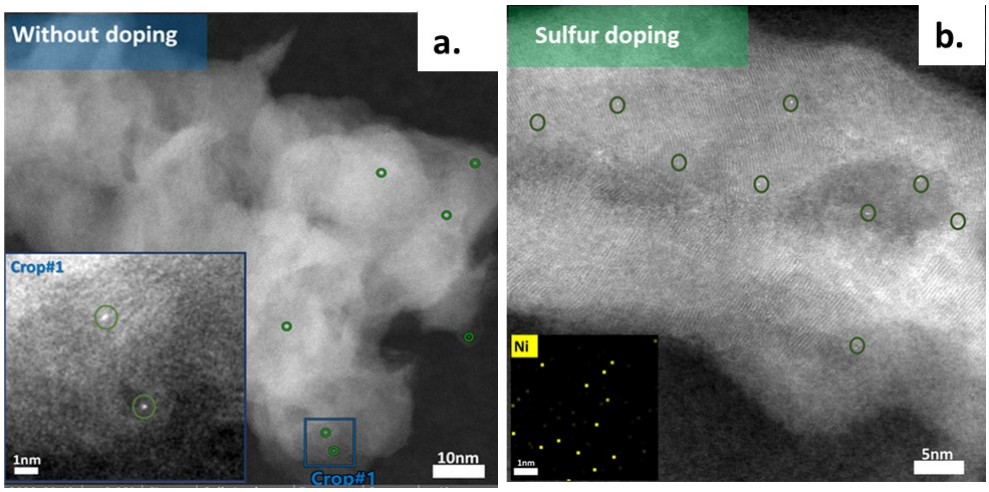

Figure S6. *Aberration-corrected high-resolution transmission electron microscopy (HRTEM) images of the delaminated electrodes (2h growth) showing SACs on the carbon: (a) non-doped (left) and (b) sulfur-doped (for 1 h, right).*

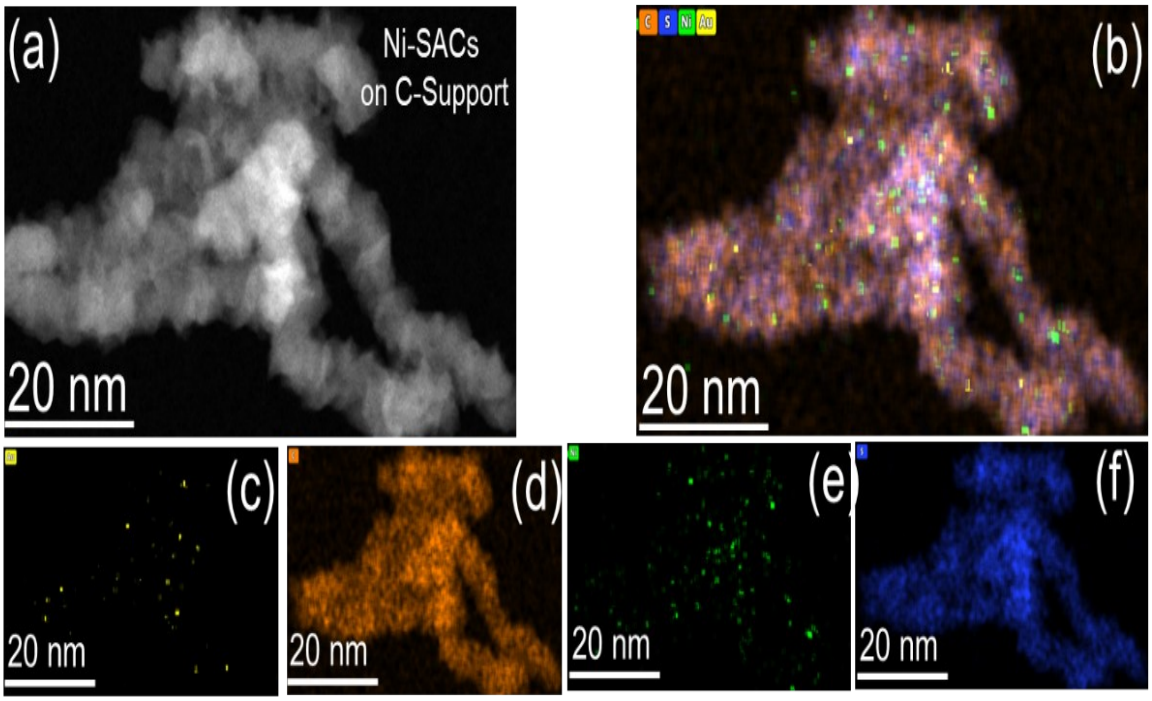

Figure S7. *Aberration-corrected HRTEM with EDS mapping of the sample with 2 h growth followed by 1 h of sulfur doping (a). Electron dispersive spectroscopy (EDS) mappings (b) shows the color mix Image of various elements, (c) stands for Au, (d) for Carbon, (e) for Ni and (f) for Sulphur. S is uniformly distributed on the as-prepared catalyst, while Ni and Au are distributed as atomic size dots.*

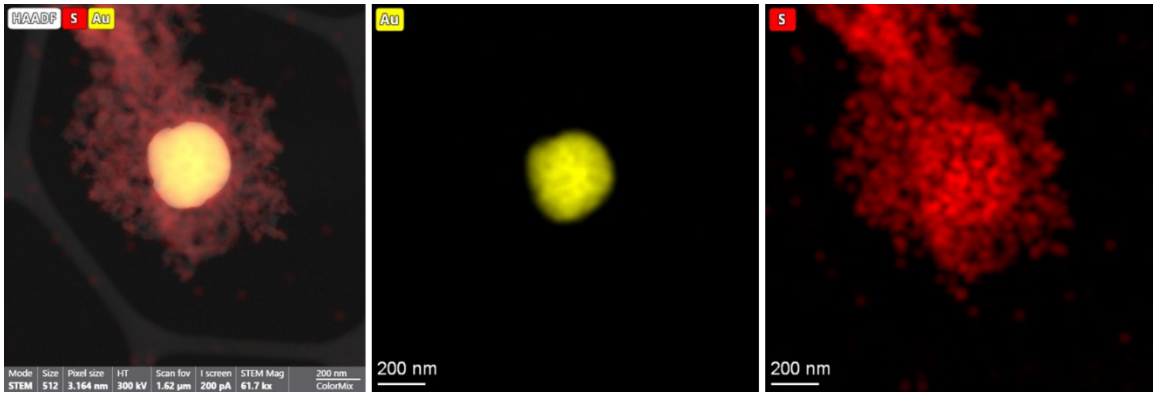

Figure S8. *HRTEM with EDS of the sample with 2 h growth followed by 1 h sulfur doping showing Au particles with a diameter of around 200 nm. HRTEM was done in a JEM 2100, JEOL (200 keV). The images were analyzed using Gatan Digital Micrograph software and processed further for quality and clarity using Image-J.*

XPS measurements were performed using a Thermo Scientific Nexsa spectrometer. The samples were irradiated with a soft X-ray source (~1.5 keV) under ultrahigh vacuum conditions (~10^{-10}–10^{-9} Torr) and their ejected photoelectrons were analyzed. Most samples showed the presence of C, O, and S, but Au was detected only in the 20 min sample. This indicates that as expected the presence of Au and Ni on the top surface of the electrode is often below the detection limit of XPS.

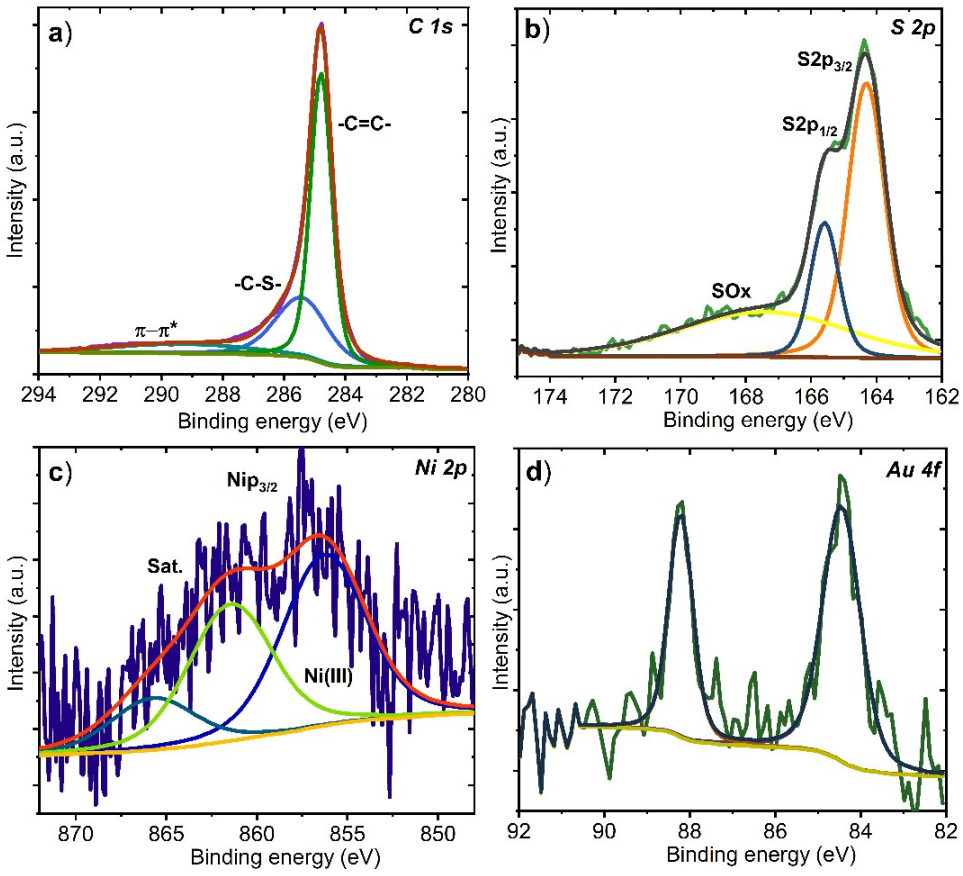

Figure S9. *XPS deconvoluted spectra of S-C_SACs: (a) C 1s, (b) S 2p, (c) Ni 2p and (d) Au 4f.*

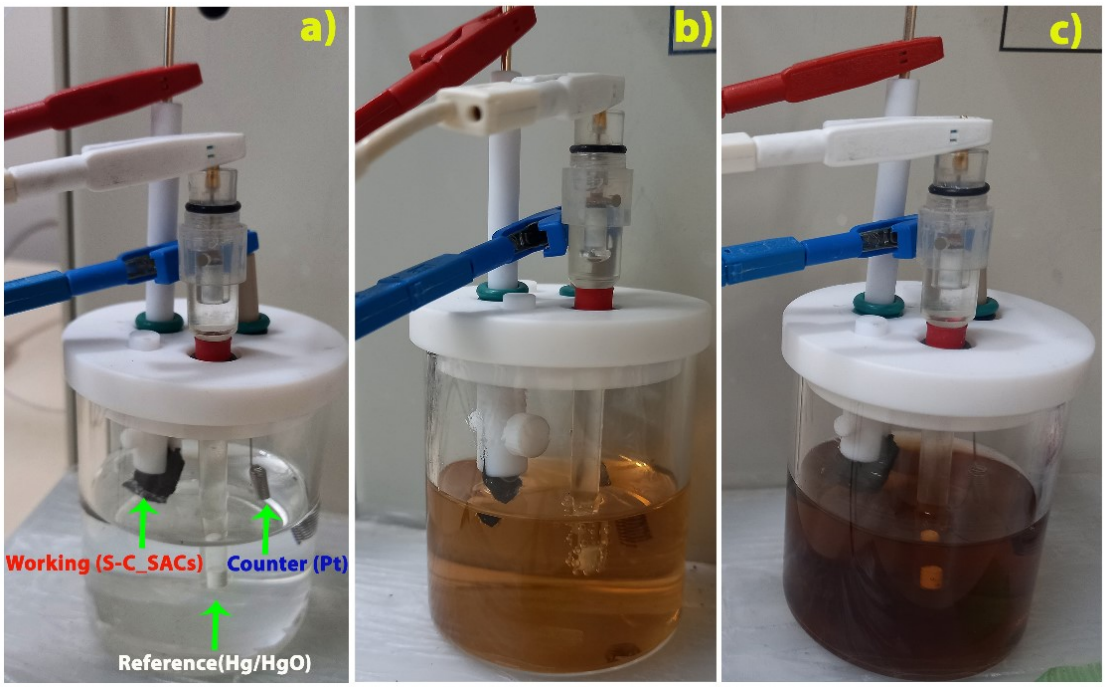

FigureS10. *Photos of the electrochemical cell (3-electrode configuration): a) fresh electrolyte (1M KOH) during OCP measurement; b) after 500 CV cycles: color changed to light brown; c) after 2000 cycles of OER: color changed to brownish red. Upon cycling the solution becomes redder indicating that the gold particles slowly dissolve from the FS electrode into the electrolyte (see UV measurements, Fig. S20).*

Electrochemical OER tests of the powder catalysts:

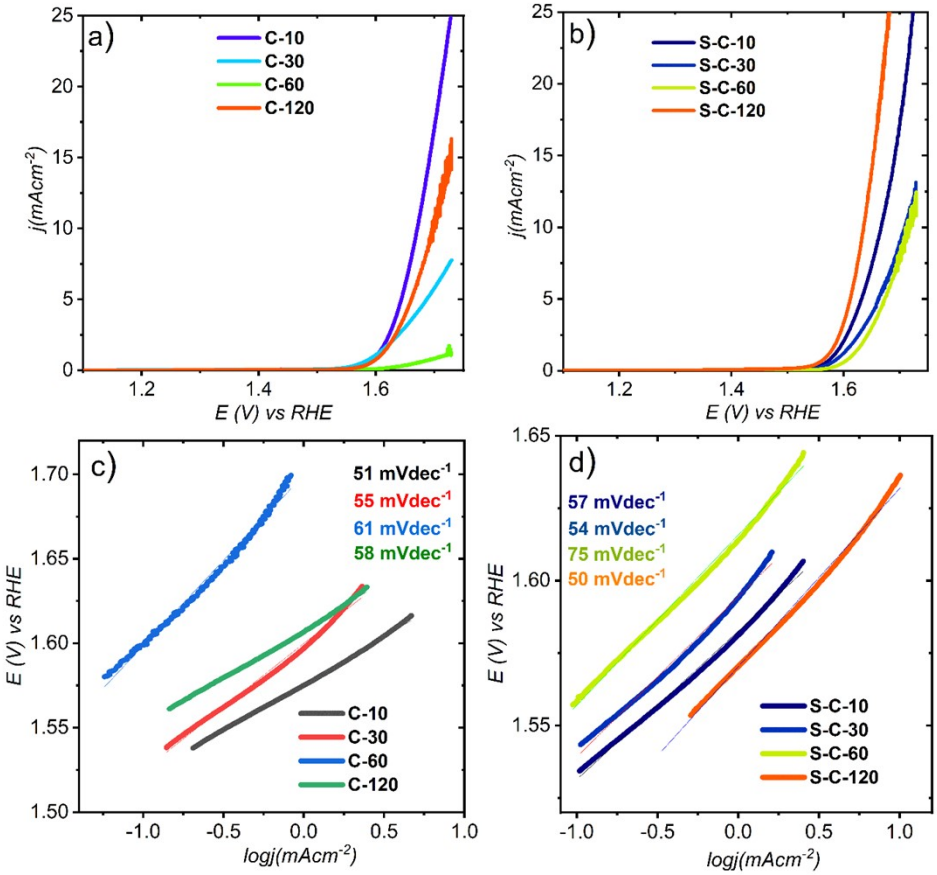

Figure S11. *Comparative linear sweep voltammetry (LSV) plots of various powder samples carried out at 5 mV/s: OER polarization curves of (a) non-doped and (b) sulfur-doped electrodes. Tafel plots of (c) non-doped and (d) sulfur-doped samples.*

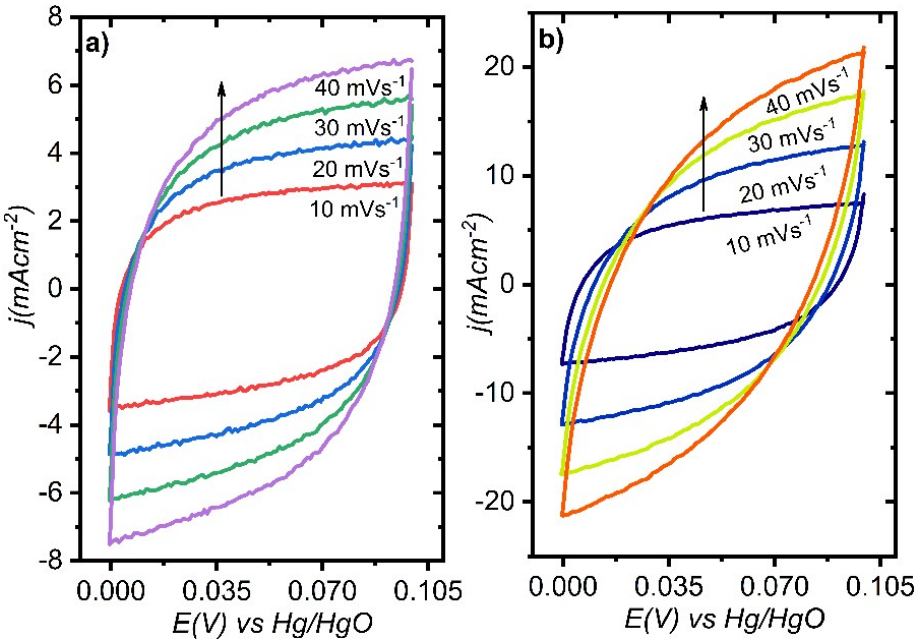

Figure S12. *Non-faradic cyclic voltammograms (CVs) at various sweep rates of (a) C-120_FS and (b) S-C-120_FS.*

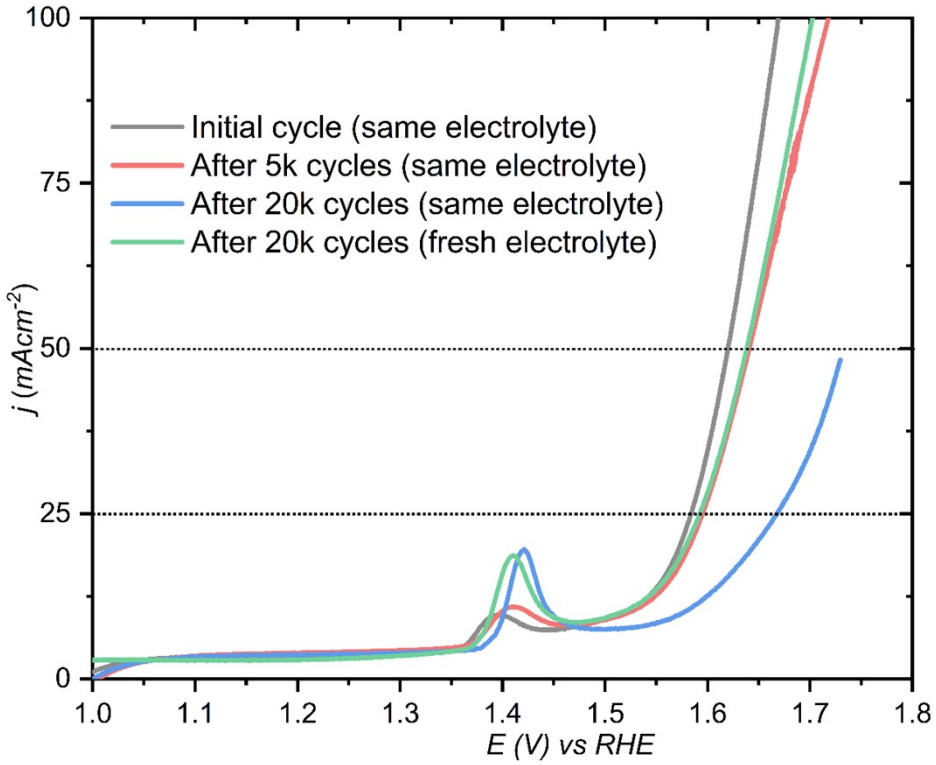

Figure S13. represents the OER durability study of the free-standing electrodes: *LSV recorded for S-C-120_FS after 5k and 20k CV cycles.*

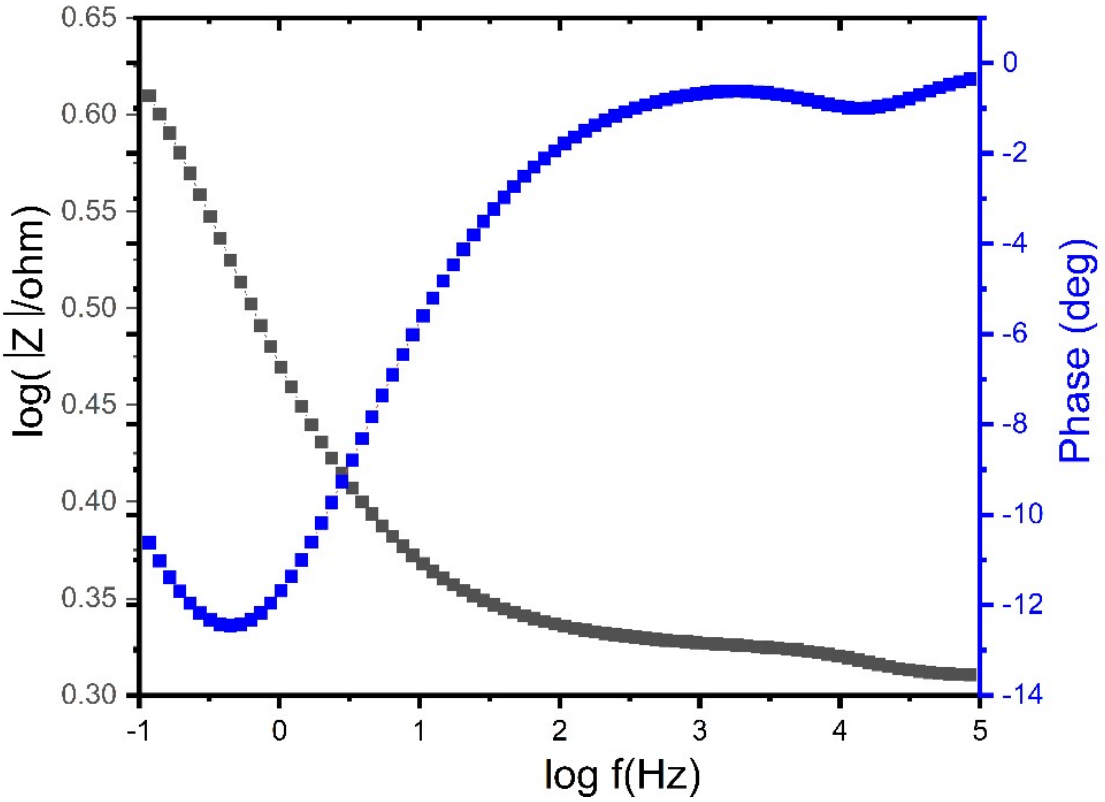

Figure S14.*Bode plot for S-C-120_FS.*

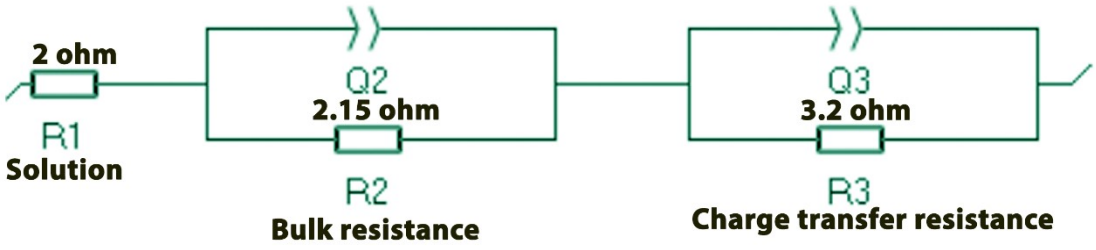

Figure S15.*Equivalent circuit diagram for the fitted Nyquist plot of S-C-120_FS.*

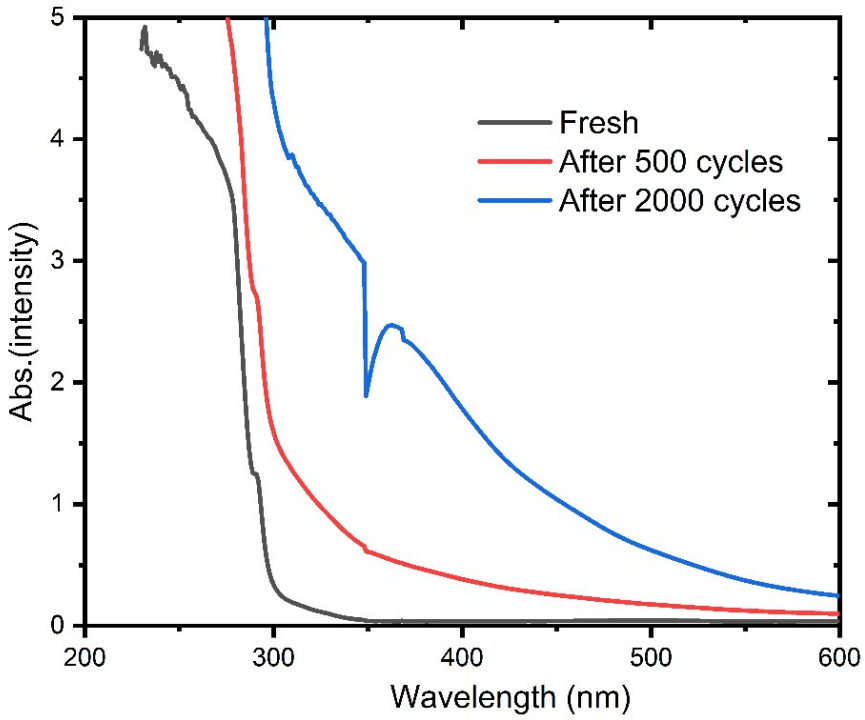

Figure S16. *UV-Vis plot of fresh 1M KOH and after 500 and 2000 OER CV cycles for sample S-C-120_FS showing the increased presence of gold in the solution as the absorbance increases.*

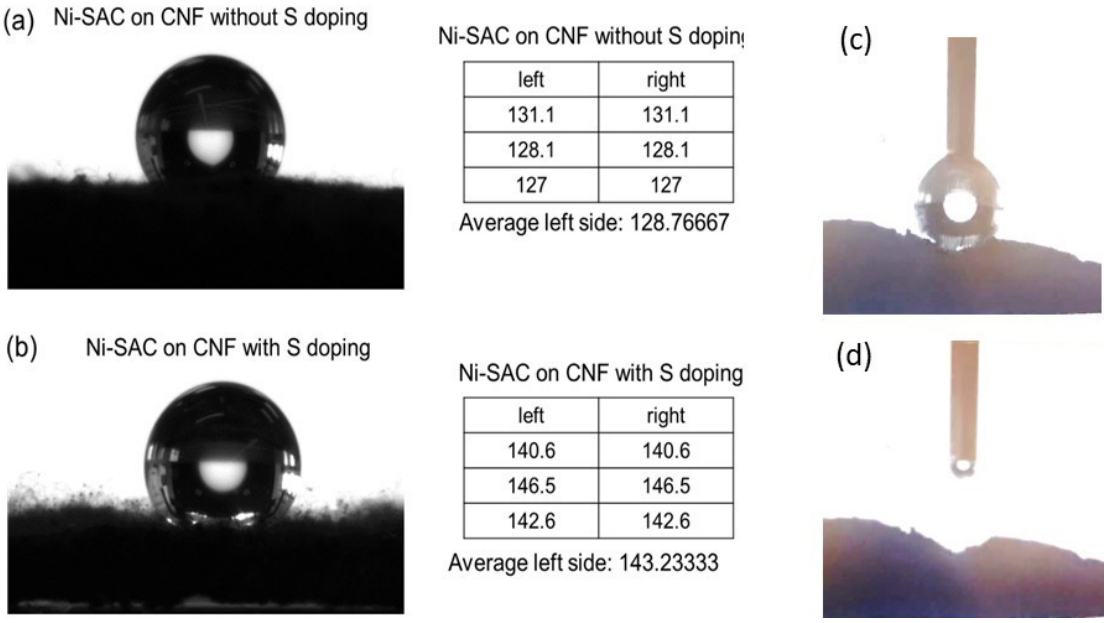

Figure S17. *Contact angle measurements of (a) C-120,(b) S-C-120. The non-doped sample shows an average angle of 128.8° compared to the more hydrophobic sulfur-doped sample with a contact angle of 143.2° (almost superhydrophobic), (c) post OER/HER S-C-120 shows the contact of water molecule on the electrode surface and (d) just by contact, the carbon surface swallowed the water bubble indicating the complete hydrophilicity character*

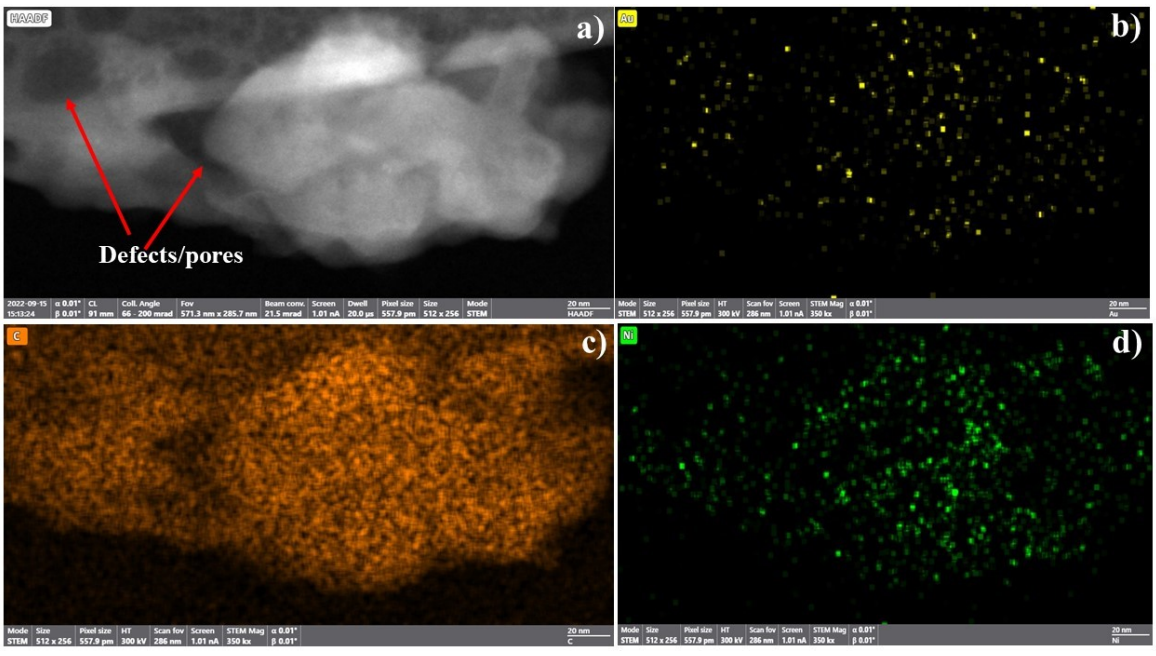

Figure S18. a) *HAADF of S-C-120_FS after 2000 OER CV cycles, b) HAADF-STEM for Au, c) HAADF-STEM represents Carbon and d) HAADF-STEM image stands for Ni.*

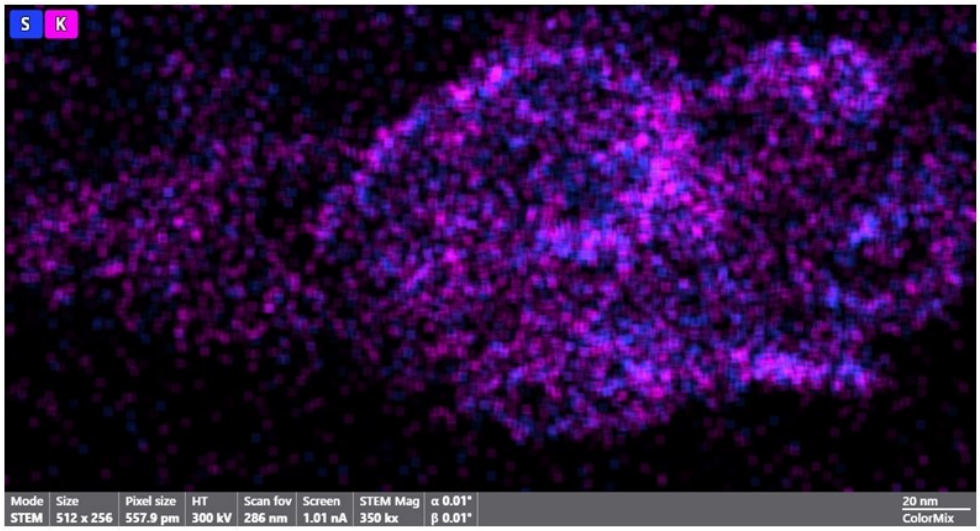

Figure S19. *HAADF-STEM of the post OER representating Sulphur and Pottasium (comes from the electrolyte, KOH solution).*

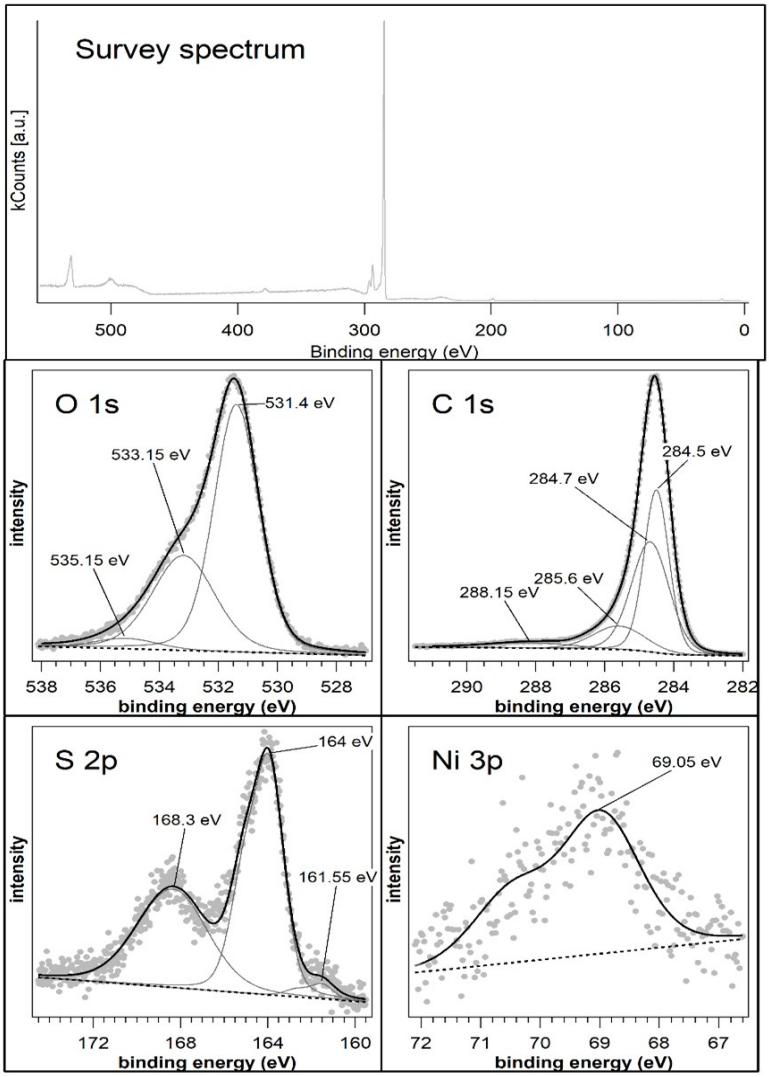

Figure S20. *Represents the survey spectra and spectra for individual elements of post OER sample, S-C-120_FS.*

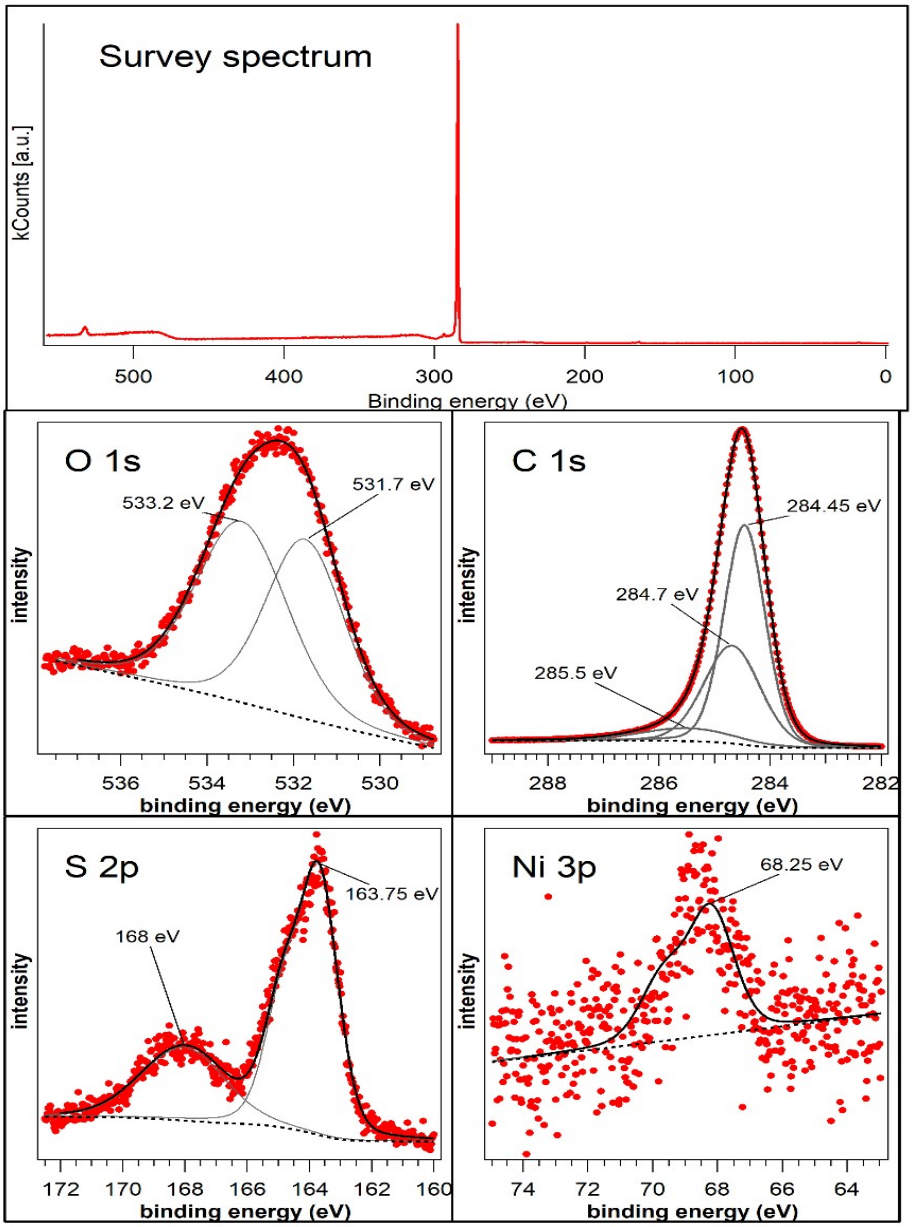

Figure S21. *Represents the survey spectra and spectra for individual elements of post HER sample, S-C-120_FS.*

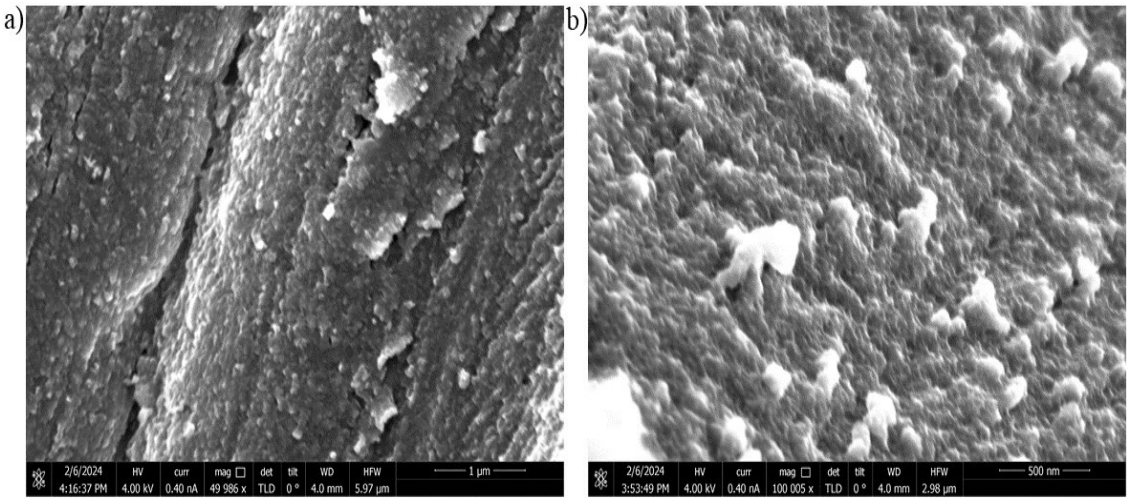

Figure S22. *Represents the HRSEM images of post OER sample (sulfur doped sample after 2h of growth) a) lower magnification image shows the formation of cracks/channels/defects and d) the highier magnification image reveling 3D patterning on the electrode surface.*

a)

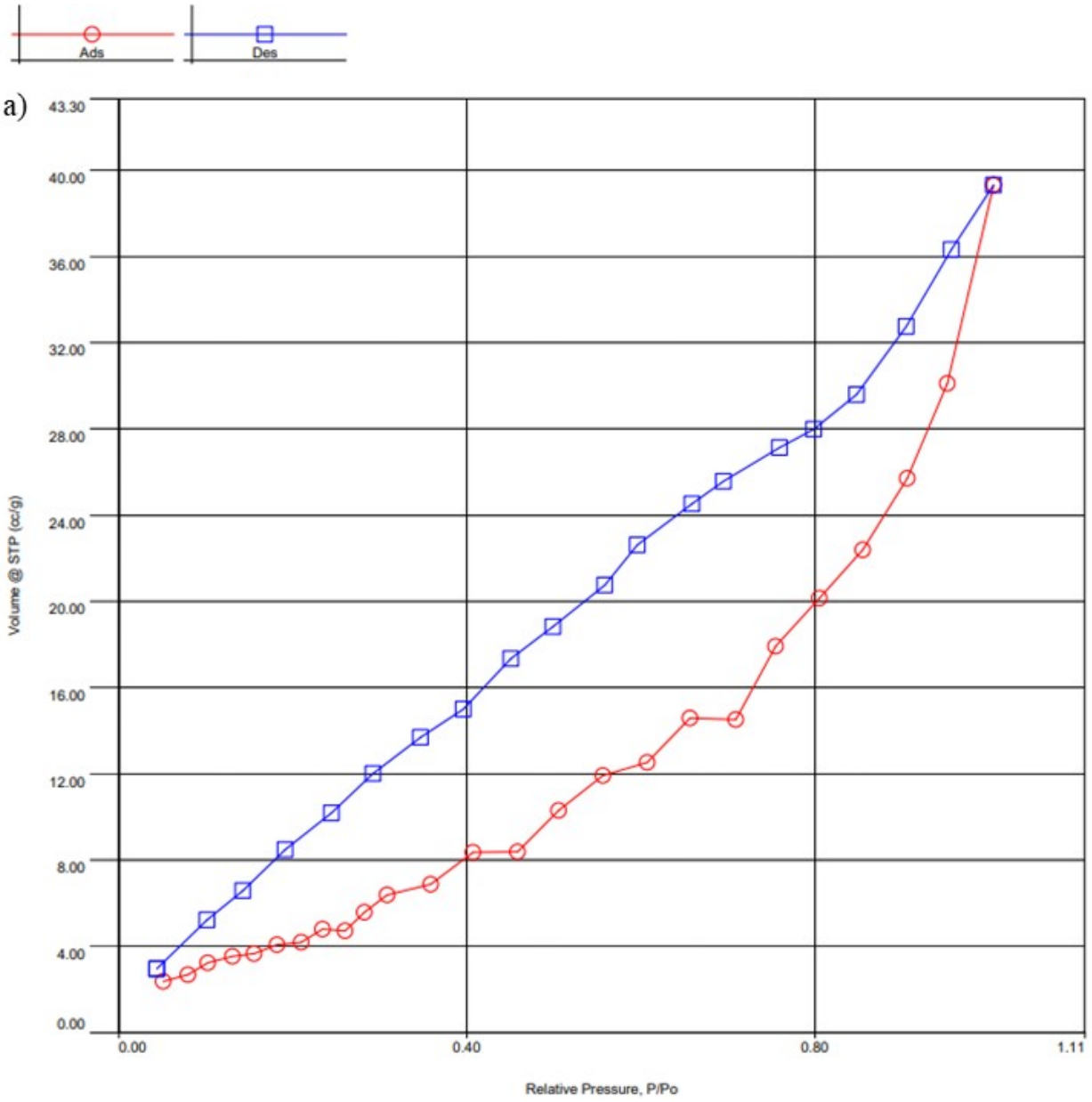
Ads
Des
43.30
40.00
36.00
32.00
28.00
24.00
20.00
16.00
12.00
8.00
4.00
0.00
Volume @ STP (cc/g)
0.00
0.40
0.80
1.11
Relative Pressure, P/Po

b)

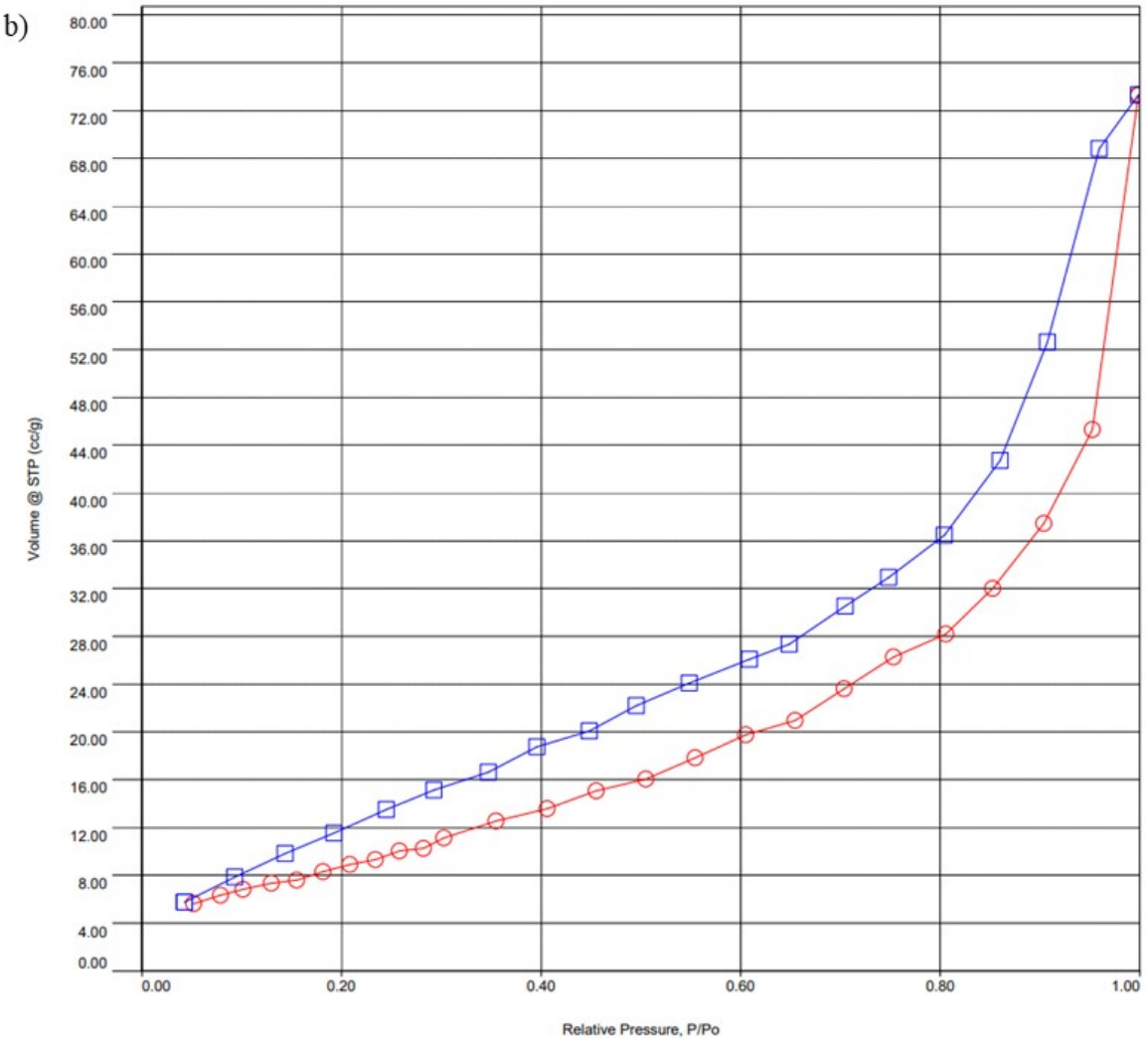
80.00
76.00
72.00
68.00
64.00
60.00
56.00
52.00
48.00
44.00
40.00
36.00
32.00
28.00
24.00
20.00
16.00
12.00
8.00
4.00
0.00
Volume @ STP (cc/g)
0.00
0.20
0.40
0.60
0.80
1.00
Relative Pressure, P/Po

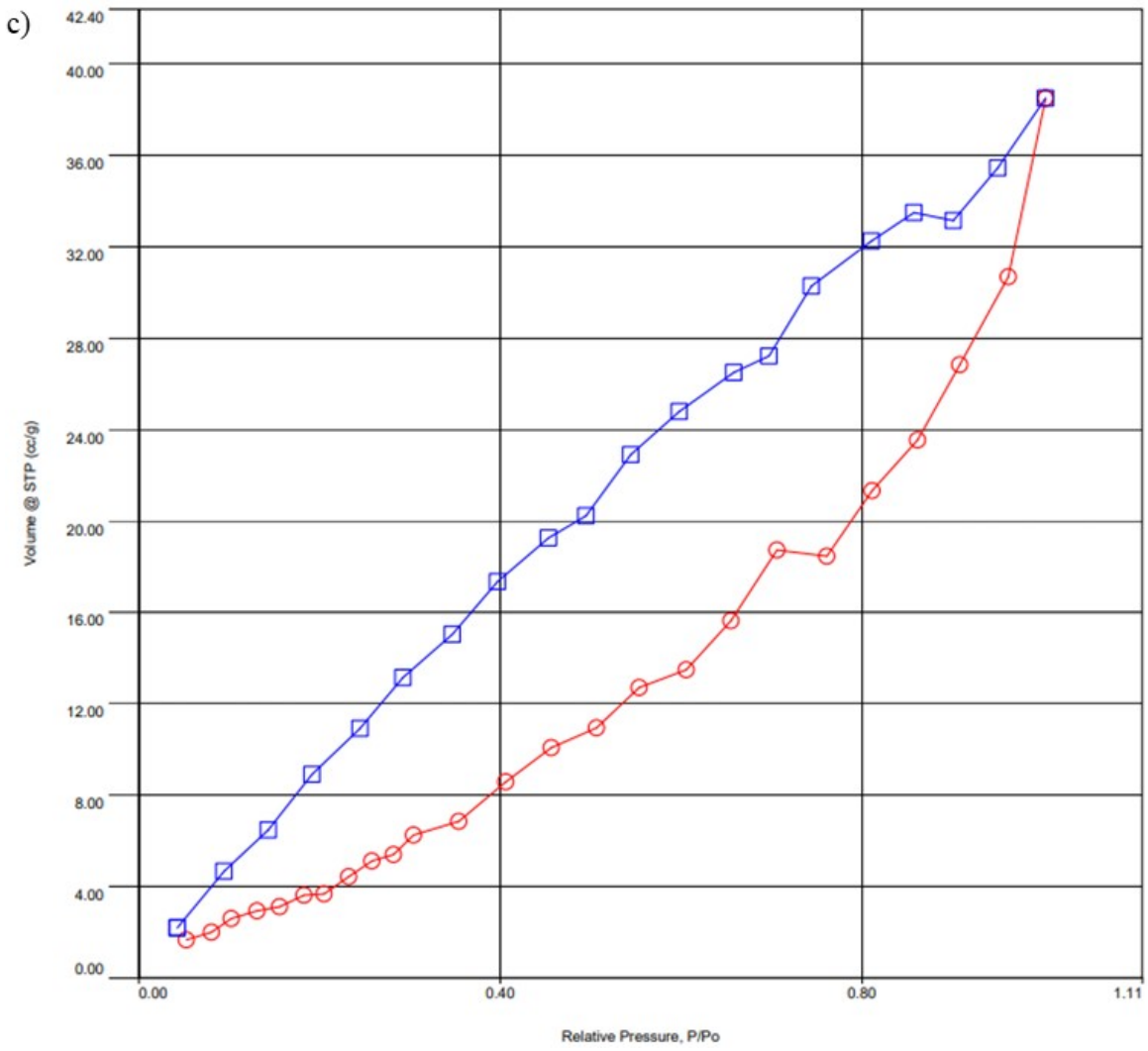

Figure S23. *BET isotherm linear plots for three samples a) S-C-120, b) S-C-120 post OER and c) S-C-120 post HER.*

Table S1: *results obtained from the BET analysis of the adsorption-desportion isotherm.*

Sample	*Avarage pore size(Å)*	*Surface area (m^2/g)*	*Total pore volume (cc/g)*	*Correlation coefficient*
S-C-120	*36.4*	*26.712*	*0.04862*	*0.955*
S-C-120 post OER	*42.99*	*31.5*	*0.06772*	*0.99*
S-C-120 post HER	*39.4711*	*24.044*	*0.04745*	*0.942592*

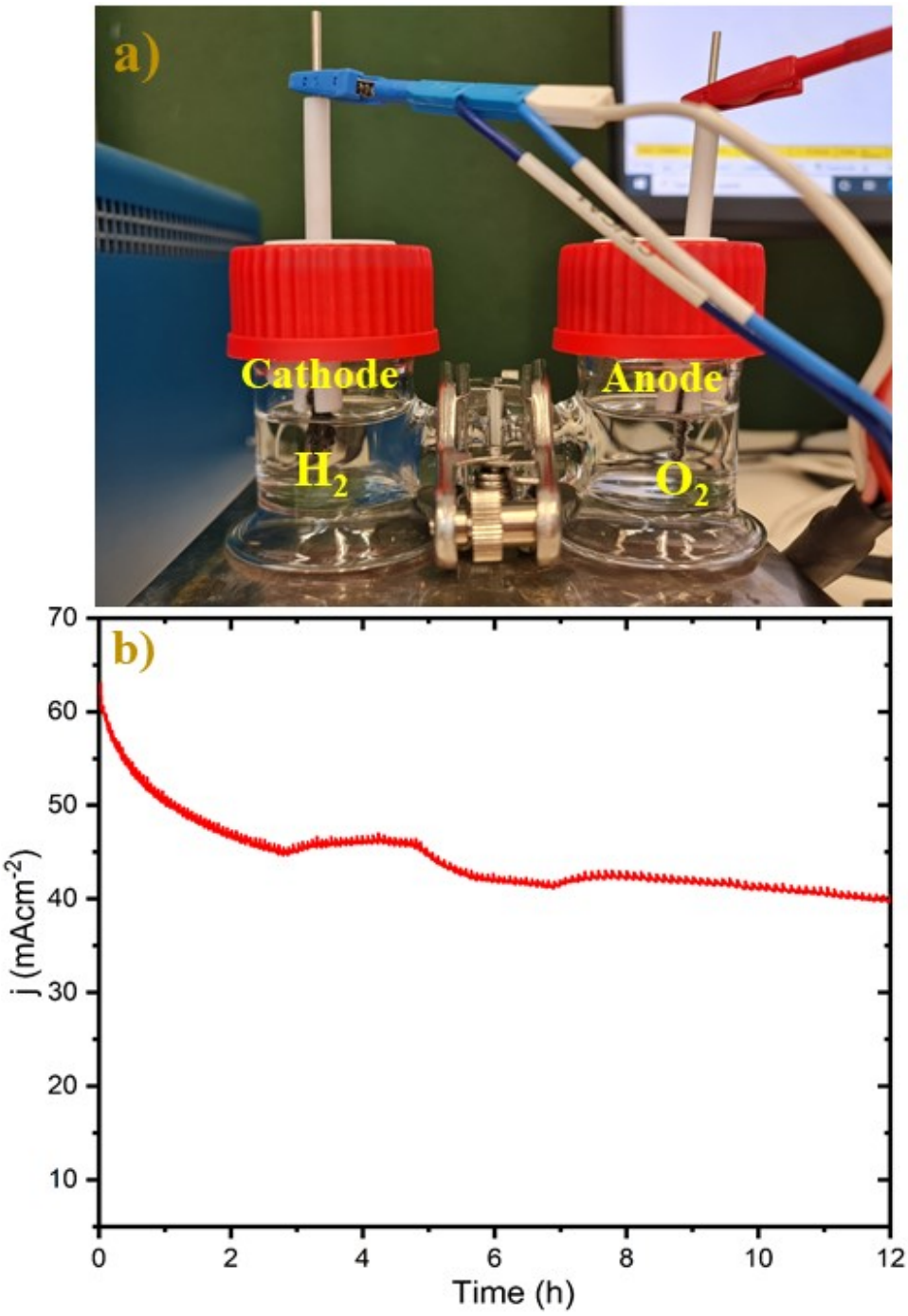

Figure S24. *a)Optical image of the two electrode setup demonstrating overwall water splitting (H_2 and O_2 gas bubbles are observed); S-C-120 FS acts as both cathode and anode where the compartments are separated by an anion exchange membrane, PiperION® b) constant electrolysis for the production H_2 shown by CA plot.*